Biomedicine & Pharmacotherapy 131 (2020) 110752

Contents lists available at ScienceDirect

Biomedicine & Pharmacotherapy

journal homepage: www.elsevier.com/locate/biopha

Original article

Protective and regenerative effects of a novel medical device against esophageal mucosal damage using *in vitro* and *ex vivo* models

Chiara Agostinis [a,*,1], Fleur Bossi [a,1], Alessandro Mangogna [a,1], Andrea Balduit [b], Micol Pacor [b], Emiliana Giacomello [b], Beatrice Belmonte [c], Daniele Greco [c], Vito Rodolico [d], Dario Voinovich [e], Francesco De Seta [a,f], Giuseppe Ricci [a,f], Roberta Bulla [b,**]

[a] Institute for Maternal and Child Health, IRCCS Burlo Garofolo, Trieste, Italy
[b] Department of Life Sciences, University of Trieste, Trieste, Italy
[c] Tumor Immunology Unit, Department of Health Sciences, University of Palermo, Palermo, Italy
[d] Department of Health Promotion, Mother and Child Care, Internal Medicine and Medical Specialties, University of Palermo, Palermo, Italy
[e] Department of Chemical and Pharmaceutical Sciences, University of Trieste, Trieste, Italy
[f] Department of Medical, Surgical and Health Science, University of Trieste, Trieste, Italy

ARTICLE INFO

Keywords:
Gastroesophageal reflux disease (GERD)
Hyaluronic acid
Rice extract
Bioadhesive polymer
Medical device

ABSTRACT

Gastroesophageal reflux disease (GERD) is a common digestive disorder that causes esophagitis and injuries to the esophageal mucosa. GERD symptoms are recurrent during pregnancy and their treatment is focused on lifestyle changes and nonprescription medicines. The aim of this study was to characterize the mechanism of action of a new patented medical device, an oral formulation containing hyaluronic acid, rice extract, and amino acids dispersed in a bioadhesive polymer matrix, by assessing its protective effects in *in vitro* and *ex vivo* models of esophageal mucosa damage. Acidic bile salts and pepsin cocktail (BSC) added to CP-A and COLO-680 N esophagus cells were used as an *in vitro* GERD model to evaluate the binding capacities, anti-inflammatory effects and reparative properties of the investigational product (IP) in comparison to a viscous control. Our results showed that the IP prevents cell permeability and tight junction dysfunction induced by BSC. Furthermore, the IP was also able to down-regulate IL-6 and IL-8 mRNA expression induced by BSC stimulation and to promote tissue repair and wound healing. The results were confirmed by *ex vivo* experiments in excised rat esophagi through the quantification of Evans Blue permeability assay. These experiments provided evidence that the IP is able to bind to the human esophagus cells, preventing the damage caused by gastroesophageal reflux, showing potential anti-irritative, soothing, and reparative properties.

1. Introduction

Gastroesophageal reflux disease (GERD) is a condition caused by the excessive spontaneous ascent of gastric contents into the esophagus [1]. The prevalence of GERD varies between 10 % and 25 % worldwide [2,3]. Important risk factors for the development of GERD are obesity, cigarette smoking, alcohol consumption, and fatty meals [3]. A higher incidence of reflux disease in pregnant women is known and reported to be up to 80 % in the third trimester, both for mechanical reasons related to compressional effects by the gravid uterus on the remaining abdominal structures, and for alterations of the motility of the lower esophageal sphincter favored by the particular hormonal pattern [4,5]. The mucosal damage caused by the refluxed gastric material is correlated to the damaging action of its individual components, such as hydrochloric acid, pepsin, and duodenal juice [6,7]. Initially, gastric hydrochloric acid and pepsin cause mucosal damage by affecting the junctions

Abbreviations: BSA, bovine serum albumin; BSC, acid bile salt and pepsin cocktail; GERD, gastroesophageal reflux disease; FBS, fetal bovine serum; F.U., fluorescent units; LPS, lipopolysaccharide; HA, hyaluronic acid; IRS, immunoreactive score; IP, investigational product; PFA, paraformaldehyde; RT, room temperature; TJP, tight junction protein; VC, viscous control; VGF®, rice extract.

* Corresponding author at: Institute for Maternal and Child Health – IRCCS Burlo Garofolo, Via dell'Istria 65/1, 34137 Trieste, Italy.
** Corresponding author at: Department of Life Sciences, University of Trieste, via Giorgieri 5, 34127 Trieste, Italy.
E-mail addresses: cagostinis@units.it (C. Agostinis), rbulla@units.it (R. Bulla).
[1] These authors contributed equally.

https://doi.org/10.1016/j.biopha.2020.110752
Received 15 June 2020; Received in revised form 26 August 2020; Accepted 10 September 2020
Available online 19 September 2020

between the esophageal epithelial cells, thus increasing the paracellular permeability and dilating intercellular spaces. Following the increased paracellular permeability, a large amount of hydrogen ions diffuse into and acidify the intercellular space; at the same time, the diffusion of chloride ions results in an osmotic imbalance [8,9]. An indirect consequence of the increased epithelial permeability is the pain sensation, often occurring in most GERD patients, due to the stimulation of sensory nerves which are exposed to the irritating luminal acidity of the gastric contents flowing back into the esophagus. In addition, acidification of the intercellular space contributes to tissue injury, causing local hypoxia and cell necrosis [8,9]. The reflux of biliary material represents a further damaging event for the esophageal mucosa [6,10–12].

Currently, different drugs for GERD are used, such as *e.g.* type 2 histamine receptor antagonists, proton pump inhibitors, relaxation reducers of the lower transient esophageal sphincter, prokinetic and protective of the mucosa [2,13]. Among over-the-counter treatments, that are miscellaneous herbal or other natural remedies, a new patented medical device based on a combination of hyaluronic acid (HA), amino acids, and rice extract (VGF®) dispersed in a bioadhesive polymer matrix may constitute a modern approach to GERD cardinal symptom relief. The investigational product (IP) is designed to reduce gastro-esophageal reflux symptoms by exerting multiple mechanical actions on the esophageal surface. Each component was selected according to its physicochemical properties, as well as its biological activity. HA is successfully used against inflammation and ulcerative lesions of the mouth (*i.e.*, aphthae, stomatitis), rapidly reducing pain and promoting healing [14]; amino acids like proline, hydroxy proline, and glutamine may be useful for sustaining the physiological repairing processes of epithelial cells when barrier function is impaired, for example, in cases of inflammation or irritation [15]; and rice (*Oryza sativa*) extract is rich in nutrients and compounds exerting soothing, antioxidant, and protective effects [16].

Considering the interesting physicochemical and curative properties of the singular natural components mixed in the IP, the aim of the current study was to assess the adhesive and protective effects of this product in two *in vitro* models of human esophageal cells, focusing on the comprehension of the mechanisms involved in its capability to reduce irritation and to sustain the physiological regenerative processes of damaged esophageal epithelium. As compared to previous works, we used the perfusion of acid solutions with pepsin and bile salts to induce mucosal lesions. Moreover, the protective effects of the IP were assessed in an *ex vivo* esophageal model collected from rats.

2. Materials and methods

2.1. Reagents and antibodies

Acid bile salt and pepsin cocktail (BSC) was used to induce *in vitro* lesions similar to those found in the esophageal tissue of patients with esophagitis and GERD. BSC was prepared with 170 μM glycocholic acid, 25 μM taurocholic acid, 100 μM deoxycholic acid, 25 μM chenodeoxycholic acid, and 50 μM glycodeoxycholic acid (all from Sigma-Aldrich, Milan, Italy); pH 2.5. Before using the solution, we added 0.25 % of freshly prepared pepsin (Sigma-Aldrich).

The IP is a patented medical device (class IIa) developed by Giellepi S.p.A. Health Science (Lissone, MB, Italy). The product contains hyaluronic acid, amino acids (*i.e.*, proline, hydroxyl–proline, glutamine), and rice extract (VGF®) dispersed in a bioadhesive polymer matrix that binds to the esophageal epithelial cells and prolongs the contact of the components with the target tissue. Viscous control (VC) is a water-based dispersion containing xanthan gum. Both IP and VC present a viscosity of 850 cPs and pH 5.

Primary antibody anti-tight junction protein (TJP)-1 was purchased from Sigma-Aldrich. Anti-rabbit IgG-FITC conjugated was purchased from Jackson Immunoresearch (ListerFish).

Table 1
Immunoreactive score (IRS) [17], commonly used for immunohistochemical evaluation.

0 = No positive cells 0 = no color reaction	1 = <10 % positive cells 1 = mild reaction	2 = 10 %–50 % positive cells 2 = moderate reaction	3 = 51 %–90 % positive cells 3 = intense reaction

2.2. Cells

CP-A (KR-42421) cells, a human esophagus immortalized cell line (epithelial cells immortalized with hTERT), were purchased from ATCC and maintained in culture using MCDB-153 medium (Sigma-Aldrich), supplemented with hydrocortisone, epidermal growth factor, bovine pituitary extract, and 10 % fetal bovine serum (FBS). Culture medium was changed every 48–72 h. CP-A cells were sub-cultured after partial digestion with 0.25 % trypsin and EDTA in Ca^{2+}/Mg^{2+}-free Dulbecco's phosphate buffered saline (DPBS).

The COLO-680 N cell line, purchased from CLS (ref. 330464), was established from human esophageal squamous-cell carcinoma. Culture medium (RPMI 1640 medium supplemented with L-glutamine and 10 % FBS) was changed every 48 h and the cells were sub-cultured after partial digestion with 0.25 % trypsin and EDTA in Ca^{2+}/Mg^{2+}-free DPBS.

Barrett's esophagus cells (CP-A) and human esophageal squamous-cell carcinoma (COLO-680 N) provided an ideal model of human esophageal mucosa through which it was possible to test the evolutionary dynamics of GERD.

2.3. Binding assay

CP-A cells were seeded in a 96-well plate until confluence and formation of a monolayer (usually after 48–72 h of culture). Both IP and VC were mixed with a solution of 0.1 % bromophenol blue in PBS and vortexed. The culture medium of CP-A was removed and replaced with DPBS +0.7 mM Ca^{2+}/Mg^{2+}, and then incubated with different concentrations of labeled IP and VC (50 %, 25 %, and 12.5 % in DPBS +0.7 mM Ca^{2+}/Mg^{2+}) for different times (1, 5, 10, 20, 30, 60, 120, and 180 min) at room temperature (RT). Cells incubated with unstained IP were considered as a negative control. The adhesion/binding of stained IP, or VC, was evaluated with the ELISA reader (O.D. 570 nm) after 1, 2, 3, or 4 washing steps with DPBS +0.7 mM Ca^{2+}/Mg^{2+}.

2.4. Epithelial permeability assay

CP-A cells (5×10^4) were seeded onto the polycarbonate insert of a 24-well Transwell system (Costar, 6.5-mm diameter, 3-μm-diameter pores) and used after reaching confluence. IP or VC was added to the wells (25 %), and after 30 min of incubation, FITC-bovine serum albumin (BSA) (1 mg/mL; Sigma-Aldrich) was added to the upper chamber. The fluorescence intensity in the lower chamber was evaluated immediately, as well as after 15 and 30 min of stimulation with BSC or bacterial lipopolysaccharide (LPS). The fluorescence intensity was measured using Infinite200 (Tecan) and expressed as fluorescent units (F.U.). The F.U. in the lower chamber provided indications about the permeability and integrity of the cell layer.

2.5. Immunofluorescence of Tight Junctions (TJ)

Confluent monolayers of CP-A or COLO680 N cells on 1.2-cm-diameter glass coverslips were exposed to different experimental treatments: 25 % IP, 25 % VC for 1 h at 37 °C, 5 % CO_2. After this pre-incubation, the cells were treated with BSC for 3–4 h. Coverslips were transferred into a humidity chamber, washed twice with DPBS, and fixed with 3 % paraformaldehyde (PFA) for 15 min at RT in darkness. Coverslips were

washed two more times with DPBS + 0.1 % Tween, and then treated with 1 % BSA, 0.1 % Triton, and 50 mM glycine in DPBS in order to perform blocking, permeabilization, and quenching simultaneously, for a duration of 30 min at RT. Cells were incubated with primary antibody anti-TJP1 (1:200) in DPBS + 1 % BSA for 1 h at RT. After washing with DPBS + 0.1 % Tween, cells were incubated with anti-rabbit IgG-FITC conjugated in DPBS + 1 % BSA for 30 min at RT in darkness. Finally, the coverslips were washed once in distilled water, air-dried, and then transferred onto a slide with a drop of fluorescence mounting medium (Dako). Mounted coverslips were examined, in a blinded fashion to ensure lack of bias, under a Leica AF6500 microscope using LAS software (Leica). The same experiments were also performed with COLO-680 N cells. To quantify the tight junction organization or disorganization after treatment, we utilized an immunoreactive score (IRS) [17], which is commonly used for immunohistochemical evaluation. For each slide, we analyzed three different visual fields of the microscope, attributing a score as described in Table 1.

2.6. Real-Time Quantitative PCR (RT-qPCR)

CP-A and COLO-680 N esophagus cell lines were seeded in a 24-well plate and incubated with IP or VC (1:4) for 1 h at 37 °C in a 5 % CO_2 incubator. Then, treated and untreated cells were incubated with BSC for 4 h. Stimulation with bacterial LPS (500 ng/mL) for 6 h was considered as a positive control. Total RNA was isolated by Total RNA Purification Kit (Norgen Biotek Corp.) and gene expression for pro-inflammatory cytokine IL-6 and chemokine IL-8 was evaluated by RT-qPCR.

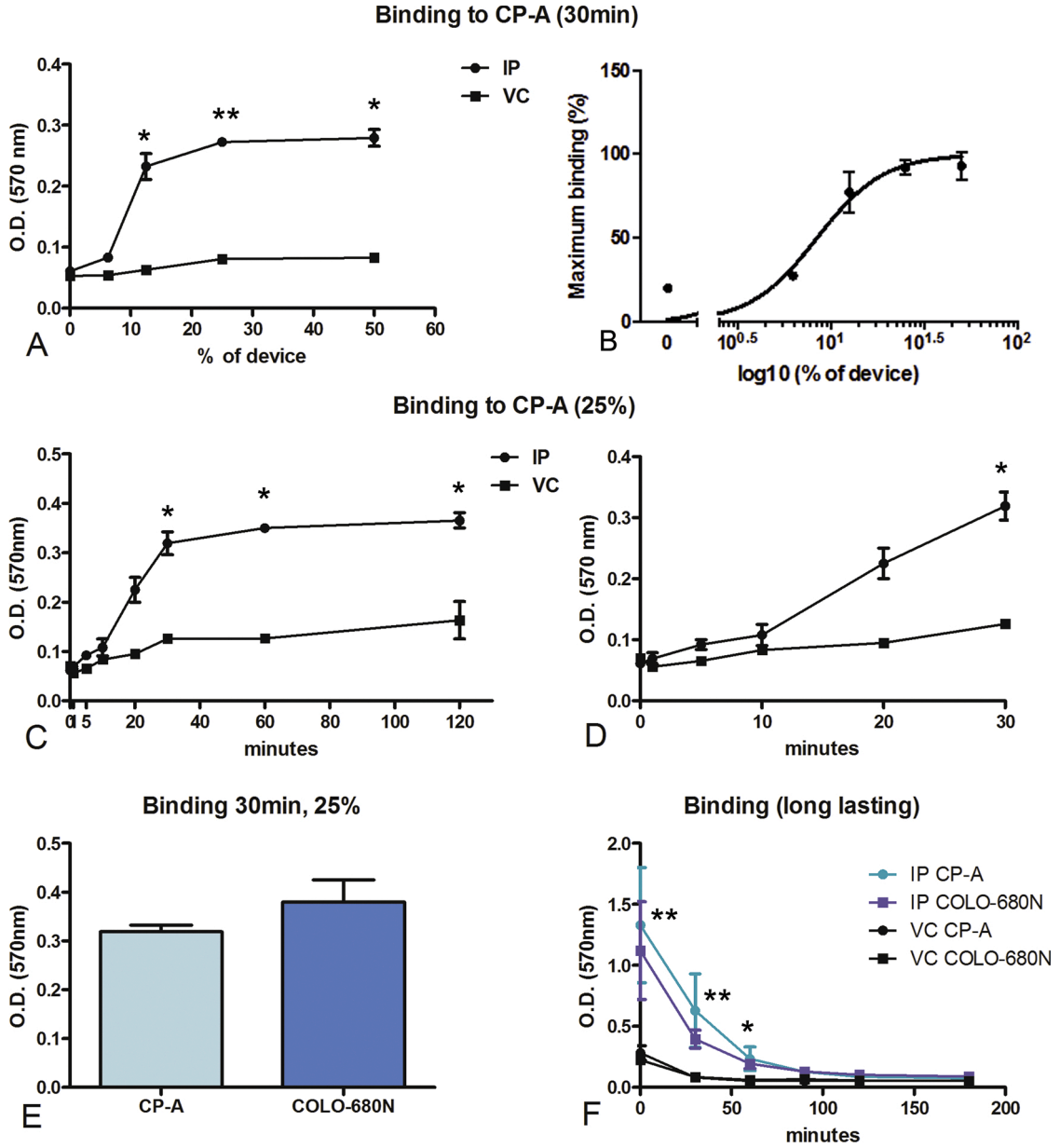

Fig. 1. Dose response and time course of the investigational product (IP) and viscous control (VC) binding to CP-A cells (A–D) and to COLO-680 N (E); extended experiments for binding of the IP to CP-A and COLO-680 N cells (F). Different concentrations of labeled IP or VC (A,B) and different incubation times (C,D) were evaluated by the ELISA reader (optical density, O.D. 570 nm). The binding plateau was observed at 25 % dilution of IP after 30 min of incubation. The binding assay was performed also on COLO-680 N after 30 min of incubation (E). The data presented in graph (F) show the results of the extended experiments, after removal of the unbound labeled IP, until 180 min of evaluation. The experiments were run in triplicate and repeated three times. The results are expressed as mean ± standard error. * $p < 0.05$; ** $p < 0.01$.

2.7. Scratch assay

Confluent monolayers of COLO-680 N esophagus cells, cultured in a 24-well plate, were scraped with a pipette tip and, after washing twice with PBS, were incubated in medium with or without BSC. After 2 h of incubation (at 37 °C in a 5 % CO_2 incubator), 25 % of IP or VC was added and incubated for 3 h at 37 °C in 5 % CO_2. Wound closure was evaluated immediately after treatment (time 0) and up to 24 h. Images were generated by the inverted microscope TE-2000U (Nikon), in the Optical Microscopy Center of the University of Trieste, Life Sciences Department, funded as described at www.units.it/confocal. The use of time-lapse microscopy allowed collecting images from the same area of interest at time 0 and after 24 h by recording spatial information. The images were analyzed by ImageJ2 software [18].

2.8. Apoptosis assay

Both esophagus cell lines seeded onto 96-well plates were allowed to grow to up to 80 % of confluence and were incubated first with BSC for 1 h and then with the IP or VC (25 %) for 4 h. Subsequently, 5 μM of CellEvent Caspase-3/7 Green Detection Reagent (Life Technologies) was supplied to the cells. Activation of caspase-3 or caspase-7 in cells undergoing apoptosis caused the cleavage of the reagent (DEVD peptide) and its consequent binding to DNA, producing a fluorogenic signal characterized by absorption/emission maxima of 502/530 nm. Fluorescence values were acquired by TECAN Infinite200, and 0.5 mM H_2O_2 was used as positive control of apoptosis.

Apoptosis was also evaluated through TUNEL assay. TUNEL assay was performed according to manufacturer's instructions (TMR red kit, cat#: 12156792910, Roche). Both esophagus cell lines were seeded onto glass coverslips and allowed to grow up to confluence. After the treatment with BSC and IP, cells were then fixed with 3 % PFA, permeabilized with 0.1 % Triton X-100 in dPBS for 2 min on ice and then incubated with In Situ Cell Death Detection Kit, TMR red (Roche) for 1 h at 37 °C in a humified atmosphere in the dark. Cells treated with 1 μg/mL staurosporine for 6 h were used as a positive control of apoptosis. After 5 min of incubation with DAPI as a nuclear counter-stain, glass coverslips were mounted and analyzed under a Leica AF6500 microscope. The percentage of TUNEL-positive cells was then determined by relating the total number of DAPI-positive nuclear staining to the total number of TUNEL-positive cells in five fields with a high-density number of cells (≥200 cells/field). The mean value was calculated for each section.

2.9. Animals

All work on animals (Wistar rats) was done according to the EU guidelines (2007/526/CE and 2010/63/UE) and the current Italian law (Decree 26/14). The study was approved by the Italian Ministry of Health, in agreement with the EU Recommendation 2007/526/CE. Animals were hosted by the University of Trieste Animal Facility (Department of Life Sciences), Italy, authorized by the Italian Ministry of Health, and breeding conditions and procedures complied with EU guidelines (2007/526/CE) and Italian law (Decree 26/14). Fifteen animals were euthanized according to an Institutional Animal Care and Use

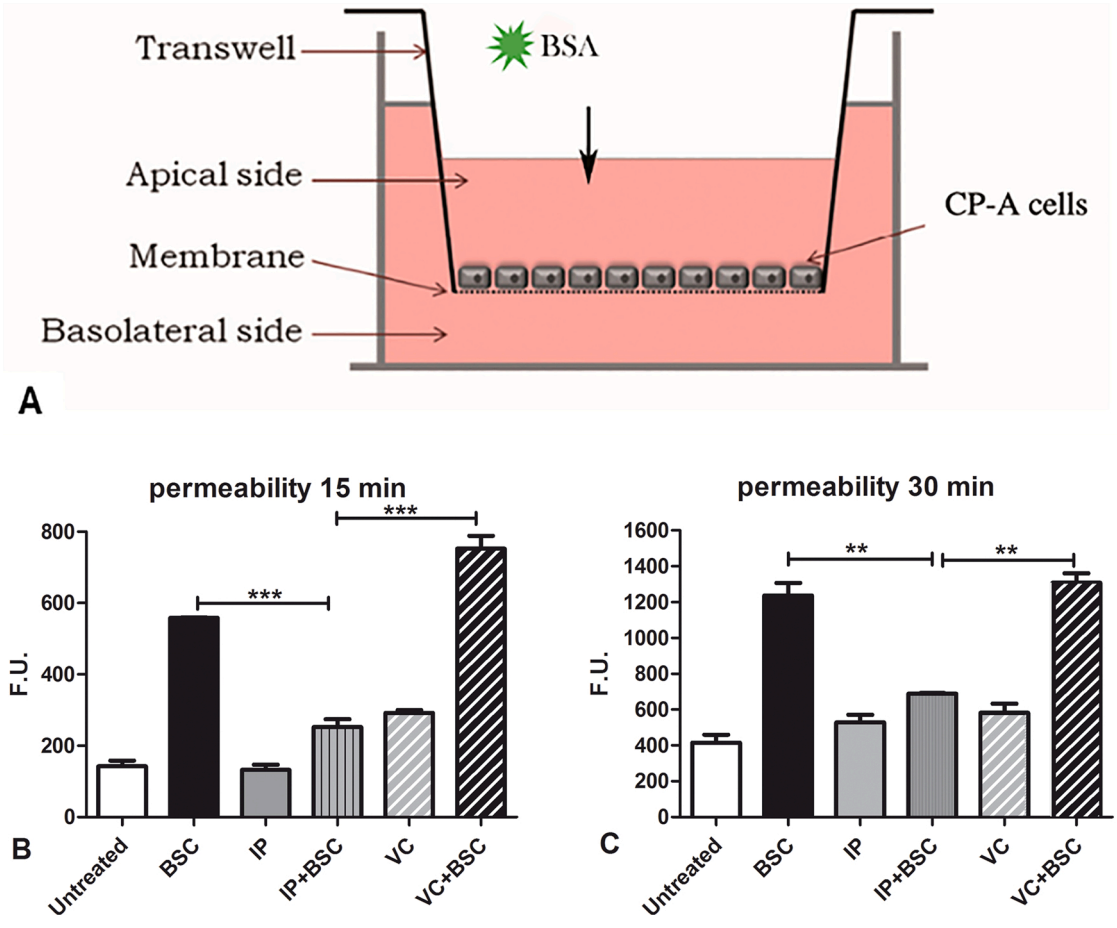

Fig. 2. Permeability assay. (**A**) Scheme of the assay. CP-A cell permeability was evaluated after 15 (**B**) and 30 (**C**) min of stimulation with acid bile salt and pepsin cocktail (BSC), by adding FITC-BSA to the upper chamber. The fluorescence intensity in the lower chamber was measured using Infinite200 (Tecan) and expressed as Fluorescent Units (F.U.). A time 0-reading of fluorescence was also carried out. Differences in permeability appeared particularly visible after 15 min of incubation. The experiments were run in triplicate and repeated three times. The results are expressed as mean ± standard error. ** $p < 0.01$; *** $p < 0.001$.

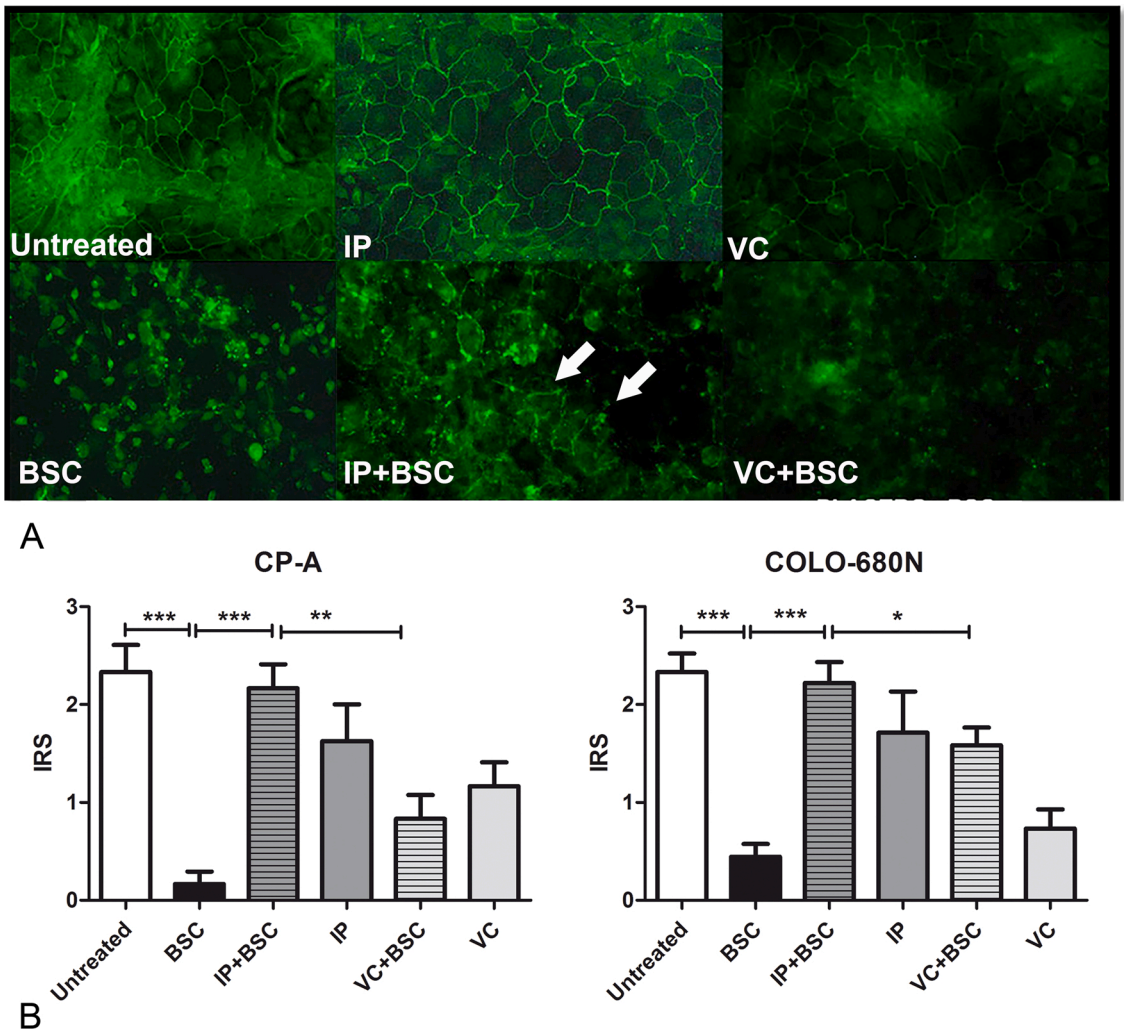

Fig. 3. Immunofluorescence assay of the Tight Junction (TJ) (**A**). The tight junction dysfunction induced by BSC incubation was prevented by the treatment with IP of COLO-680 N. To evaluate this, the cells seeded on coverslips, were stained with anti-TJP1 and secondary IgG–FITC conjugated antibodies. Coverslips were examined under a Leica AF6500 microscope using LAS software (Leica). The white arrows indicate an example of an area with well conserved TJ as a result of the protective effect exerted by IP. Quantitative analysis of TJ dysfunction (**B**). Tight junction (TJ) organization/disorganization was evaluated using an immunoreactive score (IRS) [17], which highlighted a significant protective effect exerted by IP, as compared to VC, on BSC-induced TJ disorganization. The experiments were run in duplicate and repeated three times. The results are expressed as mean ± standard error. * $p < 0.05$; ** $p < 0.01$; *** $p < 0.001$.

approved protocol; specifically, after the first step of stunning with an intraperitoneal injection of an anaesthetic dose of 40 mg/kg of ketamine and 10 mg/kg of xylazine, we proceeded with the rat sacrifice through beheading; all efforts were made to minimize suffering. The work has been performed on the explanted tissue and did not require ethical approval, as stated by the current Italian law (Decree 26/14). The entire procedure is in accordance with the regulations of the Italian Animal Welfare Act, with the relevant EU legislation and guidelines on the ethical use of animals and is approved by the local Authority Veterinary Service (rep n°65 prot n° 1493).

2.10. Ex vivo study

The rats were euthanized and the entire esophagus and stomach were clamped proximally and distally with Doyen intestinal forceps and placed in a Petri dish in a physiological solution. A syringe was used to fill the esophagus with the different solutions. The esophagus was washed twice with physiological solution and was then filled with undiluted IP or VC. After 30 min of incubation at 37 °C, the esophagus was exposed to BSC for 1 h at the concentration indicated in Section 2.1, in order to induce local irritation (inflammation/injury). At the end of the experiment, tissues were collected from the chambers and subjected to histochemistry analysis to detect epithelial damage. Tissue samples were fixed in 10 % v/v buffered formalin and were then paraffin-embedded. Four-micrometer-thick tissue sections were deparaffinized and rehydrated. Slides were stained with hematoxylin and eosin. Sections were blindly analyzed under the optical microscope, and microphotographs were collected through a color digital camera. A system of scoring was used to evaluate the tissue damage. Each histological section, stained with hematoxylin and eosin (H&E), received a score depending on its severity of evidence (0 = no damage; 1, light damage; 2, moderate damage; 3, severe damage). It consisted of assigning a numerical score for the following histological characteristics: alteration of tissue layer structure, focal destruction of tissue, intracellular and/or extracellular edema, integrity of sarcolemma, presence of vacuoles and necrosis of smooth muscle cells.

2.11. Evans blue dye method and morphological evaluation

To assess the *ex vivo* mucosal permeability, Evans Blue dye (1 % in DPBS) solution was used. Esophagi were washed twice with physiological solution and then filled with undiluted IP or VC, and after 30 min of

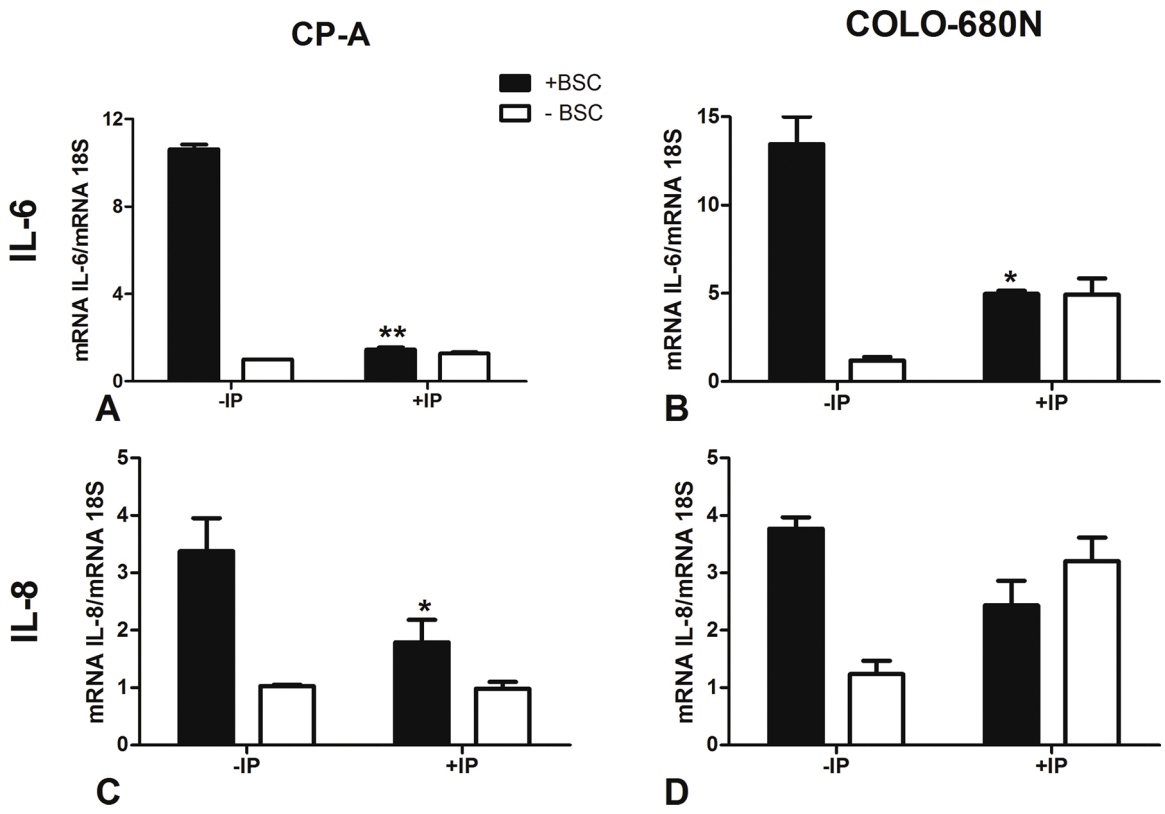

Fig. 4. Cytokine IL-6 and IL-8 expression by human esophagus cells. The pre-treatment of CP-A and COLO-680 N with the IP down-regulated the mRNA expression of IL-6 and IL-8 induced by BSC. The data were analyzed by RT-qPCR using 18S as housekeeping gene. The experiments were run in duplicate and repeated three times. The results are expressed as mean ± standard error. * $p < 0.05$; ** $p < 0.01$.

incubation at 37 °C, esophagi were exposed to BSC (or saline as control) for 1 h at the concentration indicated in Section 2.1, in order to induce local irritation (inflammation/injury). Evans Blue dye solution was injected into the esophagus and incubated for 5 min after irritant stimuli and IP treatment, as described above. The distal end of esophagus was closed with a suture thread. The esophagus was then put in a petri dish with 1 mL of physiological solution. After 5 min, the amount of Evans Blue dye that permeated outside the esophagus and that was present in the Petri dish was evaluated and quantified by the ELISA reader at 570 nm.

Frozen tissue sections were cut from Evans Blue-treated esophagi. Since the Evans Blue dye is fluorescent in the red spectrum, we analyzed the sections with both optical and fluorescence microscopy to increase the sensitivity of the analysis.

2.12. Statistical analysis

Data are reported as the mean value of two or three independent experiments ± standard error. Treatment groups were compared by analysis of variance (ANOVA), while the Bonferroni test was used for multiple comparisons. The significance criterion was set as $p < 0.05$.

3. Results

3.1. Evaluation of the Investigational Product's (IP) adhesive properties

In order to evaluate the capability of the IP to bind to the esophageal mucosa, dose response and time course experiments were conducted by adding the IP, stained with bromophenol blue, to a monolayer of CP-A or COLO-680 N. CP-A cells were incubated with different concentrations of labeled IP (Fig. 1A,B) or VC, and cells incubated with unlabeled IP were considered as negative control. As shown in Fig. 1A, IP was able to bind to CP-A cells in a dose-dependent manner, reaching saturation at 25 % dilution.

In order to define the optimal time for binding to CP-A cells, time course experiments were set up. The cells were incubated with stained IP or VC at 25 % dilution for 1, 5, 10, 20, 30, 60, and 120 min (Fig. 1C,D). The binding plateau was observed after 30 min of incubation. Since we observed large differences in terms of IP adhesion between 10 and 30 min, we wanted to investigate the binding of IP at shorter times. As shown in Fig. 1D, the binding maintained a linear trend at reduced times. These results were also confirmed with the COLO-680 N cell line (Fig. 1E).

In order to establish whether the IP, once attached, was able to remain bound, we performed an extended binding test on CP-A and COLO-680 N cells. We incubated the cells with 25 % stained IP for 30 min at RT, and after three initial washes, we measured the intensity of blue on the cells by the ELISA reader every 30 min until 180 min, removing the unbound product at every step. The IP started to detach from the cells after 60 min from the initial binding, and it was completely unbound after 120 min (Fig. 1F).

3.2. Evaluation of the IP barrier effect

The action of IP in modulating the epithelial barrier effect was initially evaluated by an *in vitro* leakage assay. These experiments provided information about the ability of the IP to preserve and/or not worsen the integrity of esophageal epithelium.

The epithelial paracellular permeability in response to BSC, with or without pre-treatment with the IP or VC, was determined by adding FITC-labeled BSA as a permeable probe in the upper chamber of a Transwell system where CP-A cells were previously seeded (Fig. 2A). The fluorescence intensity measured in the lower chamber of the Transwells at time 0 provided indications about the permeability and

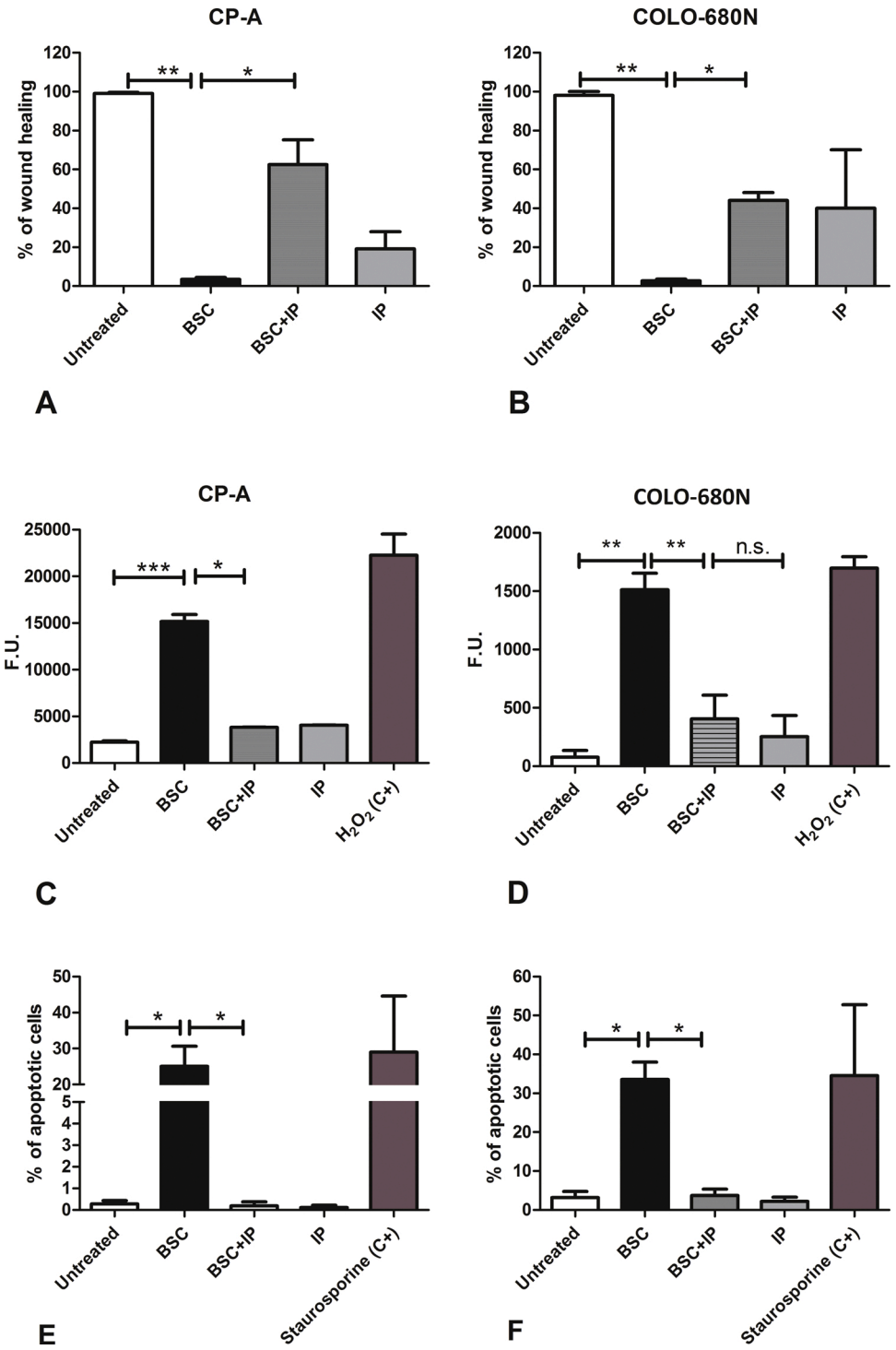

Fig. 5. Scratch assay and Apoptosis assay. Wound closure of CP-A (**A**) or COLO-680 N (**B**) scratched monolayers was evaluated under the inverted microscope TE-2000U (Nikon) and the images were analyzed by ImageJ2 software, setting the dimensions of untreated and BSC as 100 % and 0 % of wound healing, respectively. IP was significantly able to increase wound healing in BSC-treated cells. Apoptosis induced by BSC was evaluated by Caspase-3/7 activation kit (**C,D**) and resulted significantly reduced by IP treatment, indicating a reparative effect. Fluorescence values are expressed as Fluorescent Units (F.U.). BSC-induced apoptosis was evaluated also by TUNEL assay (**E,F**). Also in this case, the percentage of TUNEL positive cells resulted significantly reduced by IP treatment. Results from three experiments carried out in triplicate are expressed as mean ± standard error (SE) and compared to the results of the BSC treated cells (Mann–Whitney test). The experiments were run in duplicate and repeated three times. The results are expressed as mean ± standard error. * $p < 0.05$; ** $p < 0.01$; *** $p < 0.001$.

integrity of cell layer. COLO-680 N have been proved technically unsuitable for this kind of test because they did not form a stable monolayer even in the absence of stimuli. As shown in Fig. 2B,C, the IP (and not VC) was able to reduce the permeability effect induced by BSC up to the control (Untreated) values, particularly after 15 min of incubation (Fig. 2B).

The effect of the IP in modulating the epithelial barrier in terms of tight junction integrity was also evaluated. For an immunofluorescence evaluation of TJ proteins, esophagus CP-A or COLO-680 N cells grown on glass coverslips were exposed to 25 % IP or 25 % VC. After this preincubation, cells were treated with BSC for 3–4 h. Coverslips were stained with anti-TJP1 primary antibody and then with anti-rabbit IgG FITC-conjugated antibody. Our results indicated that IP (and not VC) partially prevents the alterations of the TJ induced by BSC treatment (Fig. 3A). The same experiments, performed also with COLO-680 N, were used for TJ quantification (Fig. 3B). To quantify TJ organization or disorganization after treatment, we used a simple method of image processing using an immunoreactive score (IRS) [17]. The graph in

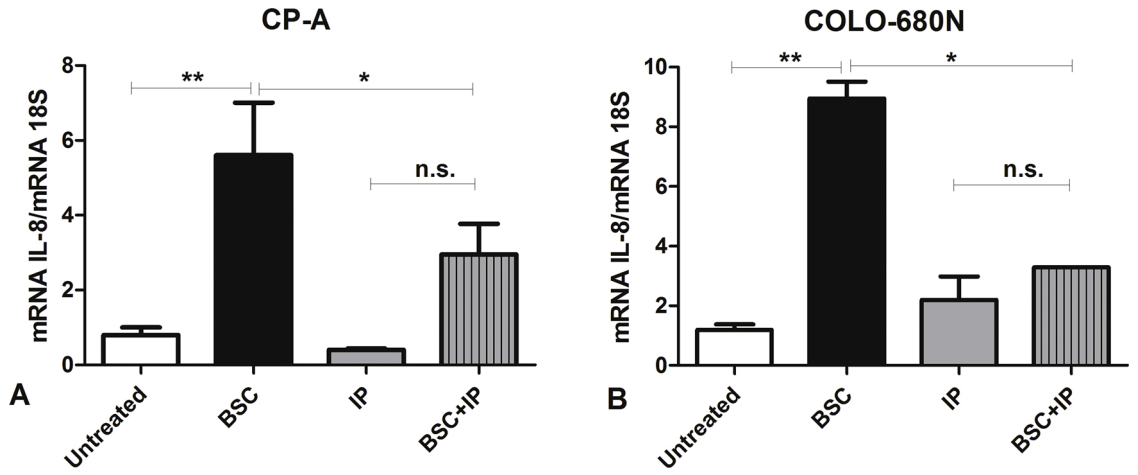

Fig. 6. Cytokine IL-8 expression of CP-A (**A**) and COLO-680 N (**B**) cell lines. Esophagus cells incubated with BSC and subsequently treated with the IP were analyzed for the expression of chemokine IL-8 by RT-qPCR. In both cell lines, the treatment with IP induced a significant down-regulation of IL-8 expression caused by BSC. The experiments were run in duplicate and repeated three times. The results are expressed as mean ± standard error. * $p < 0.05$; ** $p < 0.01$.

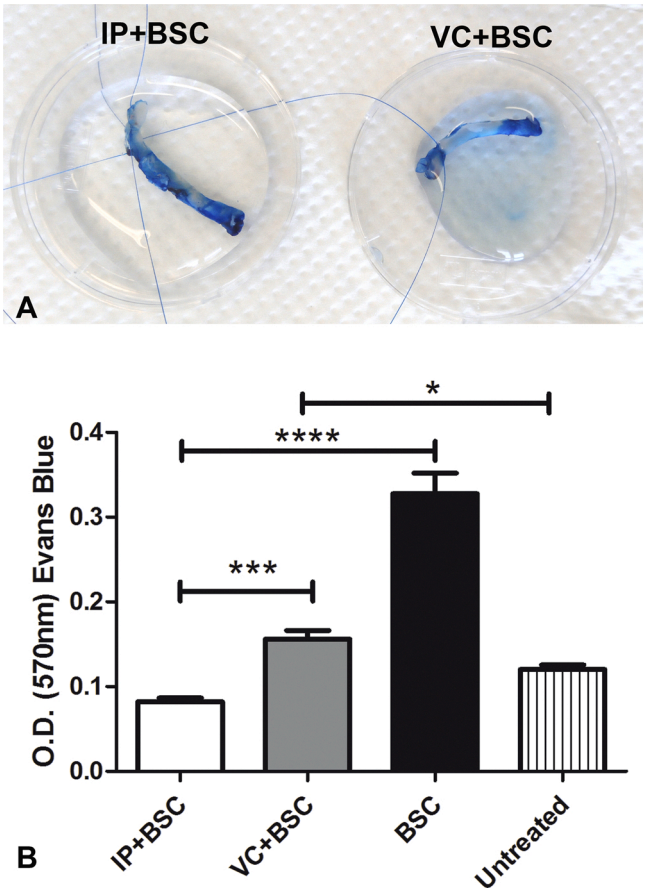

Fig. 7. Quantification of Evans Blue permeated outside the rat esophagi, after treatment with the IP (n = 3), BSC (n = 3), IP + BSC (n = 4), or VC + BSC (n = 4). In the upper panel there is a representative picture of the Evans Blue-treated and clamped esophagi after 5 min of incubation in the petri dishes with DPBS (**A**). The quantification of the dye was performed by the ELISA reader at 570 nm after 5 min of incubation (**B**). The results are expressed as mean ± standard error. * $p < 0.05$; *** $p < 0.001$; **** $p < 0.0001$.

Fig. 3B shows that the preincubation of cells with the IP was able to induce a significant protective effect for cell TJ disorganization induced by BSC as compared to VC treatment. The same results were also confirmed using CP-A cells (data not shown).

The IP barrier effect was also demonstrated by analyzing the effect on cytokine production by BSC-stimulated epithelial cells. Gene expression analysis indicated that BSC was able to induce the expression of the pro-inflammatory cytokines IL-6 and IL-8 in both CP-A and COLO-680 N cells (Fig. 4). The pre-treatment with IP significantly reduced the amount of IL-6 and IL-8 mRNA production by CP-A (Fig. 4A–C) and IL-6 expression by COLO-680 N cells (Fig. 4B–D).

3.3. Evaluation of IP reparative properties

The capability of IP to sustain the regenerative process of damaged esophageal mucosa was investigated by scratch assay. The wound healing in CP-A and COLO-680 N scratched monolayer resulted more rapid when the cells were treated with IP, in particular if the treatment was following the stimulation with BSC (Supplementary Fig. 1). The graphs in Fig. 5A,B clearly showed that the IP was able to induce a significant increase in wound healing in BSC-treated cells.

The results obtained from the scratch assay were confirmed by apoptosis evaluation, using two different assays (Caspase-activation kit and TUNEL staining). In Fig. 5C–E, the treatment of COLO-680 N and CP-A cells with BSC resulted in the induction of cell apoptosis as the positive control (H_2O_2 or staurosporine). The treatment of cells with the IP significantly reduced the amount of apoptosis induced by BSC, indicating a reparative effect.

3.4. Evaluation of IP soothing activity

Damaged mucosa is often associated with irritation and inflammation. Gene expression of chemokine IL-8 was considered as a marker of inflammatory activation. As shown in Fig. 6, a very low expression of IL-8 mRNA by resting (Untreated) cells or CP-A and COLO-680 N cells incubated with the IP was observed. Cells treated with BSC strongly increased the expression of IL-8 and, in both cell types, the IP reduced the expression of IL-8 induced by BSC stimulation.

3.5. Ex vivo evaluation of the IP barrier effect

The assessment of the efficacy of the IP in preventing esophagus mucosal permeability, induced by BSC treatment, was evaluated by *ex vivo* analysis of a rat esophageal model using the Evans Blue dye method. The permeability both in *ex vivo* and *in vitro* assays could be influenced by the mechanical barrier effect of IP, so we compared the results obtained with IP to a VC with the same barrier effect. We believe that the

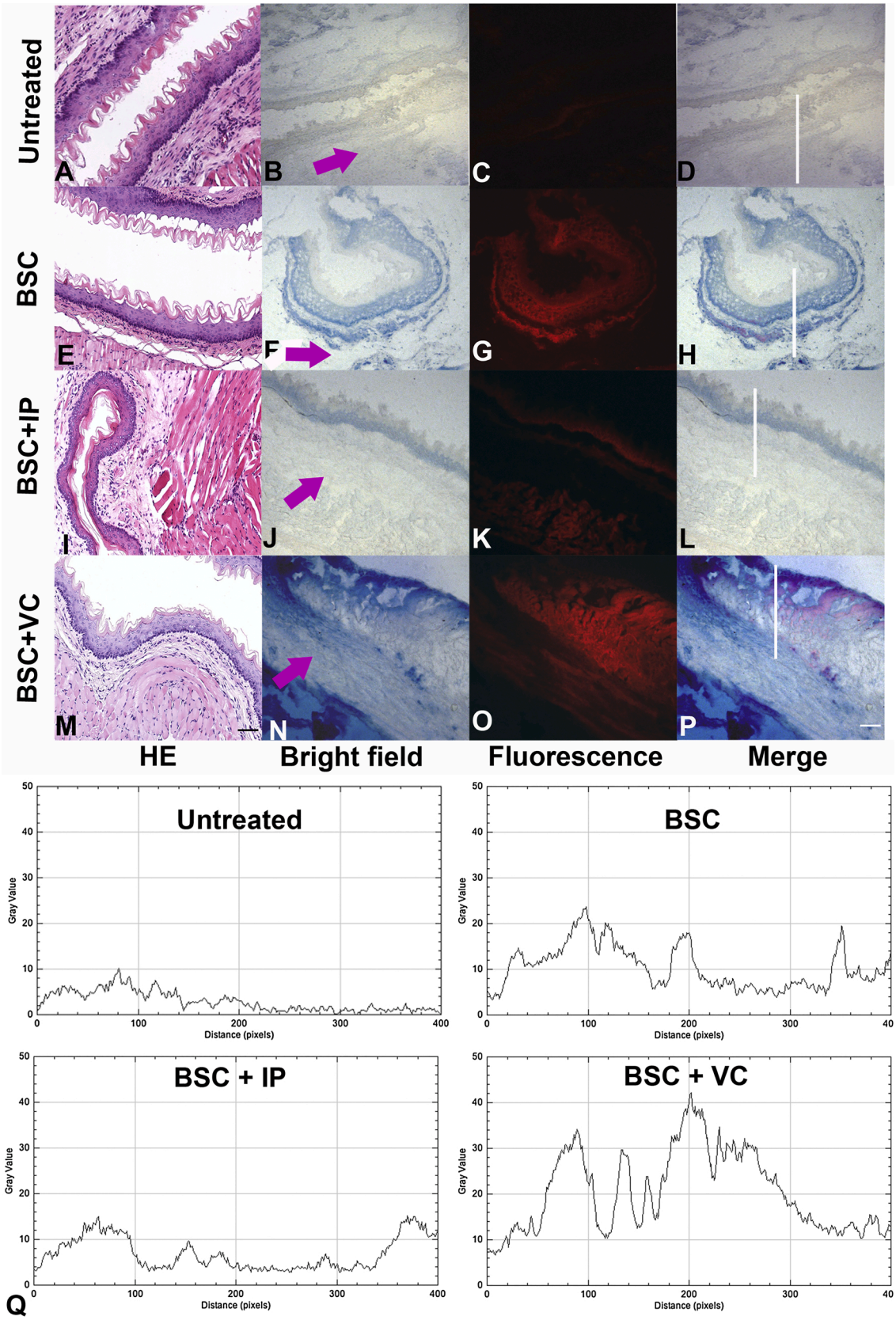

Fig. 8. Histological analyses. Rat esophagi were subjected to the indicated treatments and processed for Hematoxylin and Eosin staining (**A,E,I,M**) for histological inspection. For the Evans Blue permeability assay, tissue samples were cryosectioned and images were acquired in both the bright field panels (**B,F,J,N**) to detect the esophagus tissue and under the fluorescence panels (**C,G,K,O**) to detect Evans Blue. In each merged image panel (**D,H,L,P**), a line from the top of the esophagus epithelium to the submucosa was drawn, and the plot profile of Evans Blue fluorescence was reported for each sample panel (**Q**). The fluorescence was measured on gray scale images, and the plot profiles report fluorescence intensity as gray values. The arrow points toward the submucosa. Magnification, 200x; scale bars, 50 μm.

principal comparison in *ex vivo* experiments is IP + BSC *vs* VC + BSC, because the excised esophagus tissue, without the incubation with a dense compound (Untreated), can be permeated by the Evans blue also in resting conditions.

Esophagi filled and incubated with undiluted IP or VC were exposed to BSC to induce local irritation (inflammation/injury) and Evans Blue dye solution was injected into the esophagus. After clamping the distal end with a suture thread, esophagus was then placed in a petri dish with physiological solution (Fig. 7A) and the Evans blue permeated outside the esophagus was measured by ELISA reader (Fig. 7B). Moreover, frozen tissue sections were cut from Evans Blue-treated esophagi for a morphological evaluation.

Since the Evans Blue dye is a fluorescent molecule that allows detection of the permeability of cells and tissues in situ, the sections were analyzed with optical and fluorescence microscopy to increase the sensitivity of the analysis, and differences among the three conditions tested were identified (Fig. 7).

Cryosections obtained from the treated samples were analyzed in both bright-field, to detect the esophagus tissue, and Rhodamine filter, to detect Evans Blue. Slides were stained with H&E and three sections for each condition were blindly analyzed under the optical microscope. A semi-quantifying histological evaluation was performed (see M&M section) but the analysis of the sections indicated that no significant differences were noticed by histological inspection (Supplementary Fig. 2). As reported in Fig. 8E–H, in the BSC-treated sample, the fluorescence levels corresponding to the line drawn from the tip of the epithelium to the submucosa (arrow) indicate that the Evans Blue permeated under the epithelial layer into the lamina propria. Interestingly, when the esophagus was treated with the IP, the levels of Evans Blue that passed through the epithelial barrier were considerably reduced (Fig. 8I–L). The maximum of fluorescence measured was reduced by about 30 % as compared to BSC, and the peaks were narrower (Fig. 8Q). The treatment with VC increased both the size and the maximum intensity of the Evans Blue fluorescence of about 60 % (Fig. 8M–P).

Our results suggest that the IP was able to prevent the permeability induced by BSC, while VC displayed a higher Evans Blue permeability compared to both the IP and the BSC.

4. Discussion

Previous experimental investigations, performed on both *in vitro* [19,20] and *in vivo* animal models [21–24], have clearly demonstrated that the treatment with preparations containing HCl and pepsin may provoke a esophageal mucosal damage similar to the lesions induced by gastroesophageal reflux. However, also the reflux of biliary material represents an important damaging event for the esophageal mucosa [6,10–12]. The gastric contents can be mixed with duodenal substances following episodes of transpyloric reflux of bile and pancreatic secretions [6,10,11,25,26]. The term “bile reflux,” or more recently defined as “alkaline or weakly acid reflux,” is used to describe this process, since in addition to bile, the duodenal content contains various components which are potentially harmful [10,27–29]. However, the mechanism by which bile acids can cause mucosal damage is not completely understood. Bile acids have a cleaning power and solubilize cellular lipid membranes [30,31]. At the esophageal level, the interruption of the mucous barrier occurs due to concentrations of bile acids being lower than the level necessary to solubilize the membrane phospholipids [11,32]. Therefore, alternatively, it is believed that, thanks to their lipophilicity, bile acids can cross the mucosa, remaining trapped inside the cells following intracellular ionization, and thus reaching the high concentrations responsible for the damage [12,32].

Our work compared to previous studies emphasizes also the role of bile salts in the pathophysiological mechanisms of GERD. Indeed, we provide evidence that a new patented oral formulation, containing hyaluronic acid, rice extract, and amino acids dispersed in a bioadhesive polymer matrix, is able to adhere to human esophageal cells throughout the entire esophagus, and it is capable of preventing the damage caused not only by mere gastric content flowing back into the esophagus during gastroesophageal reflux but also by bile salts.

Exposure of the esophageal tissue to acidic and/or weakly acidic solutions containing bile salts can lead to an impairment of the barrier function and an increase in transepithelial permeability [11,33]. The permeation of harmful components of the reflux into the mucosa is prevented by the non-keratinized stratified squamous epithelium [34,35]. Using two different human esophageal cells as an *in vitro* model, we tested the protective effects of the IP after exposing the cells to the irritant stimulus BSC, an acid bile salt and pepsin cocktail used to induce lesions similar to those found in patients with esophagitis and GERD. Our experiments demonstrated the ability of the IP to reduce the permeability of the mucosa, indicating that it can preserve the integrity of the esophageal epithelium in harsh conditions, such as in the presence of BSC. Overall, the IP was able to prevent injuries caused by the BSC solution. This effect appeared to be due to a persistent adherence of the IP to the esophageal mucosa. Since the transit time of liquids through the esophagus is very short (less than 16 s) [36], a liquid formulation possessing mucoadhesive properties to adhere and coat the gastroesophageal mucosa is ideal for limiting the contact of gastroesophageal reflux with the epithelial surface [37] and as a vehicle for delivering substances for local and mechanical actions within the esophagus [38].

Several animal models have also been developed to mimic the GERD and study its mechanisms. Surgical reflux models can be categorized into four subtypes: (1) only gastric secretion reflux, (2) only duodenal secretion reflux, (3) duodenogastric reflux with “bile predominance”, and (4) duodenogastric reflux with “acid predominance” [31,32]. Surgical reflux models in mice or rats are technically challenging due to the small size and intolerance to surgical stress of small animals. In addition, they have a stratified squamous epithelium-lined esophagus, similar to the human esophagus.

In the current study, the efficacy of the IP to prevent esophagus mucosal permeability was also assessed by using an *ex vivo* rat model of esophageal damage. The results obtained with the animal model confirm that the IP strongly reduces the Evans Blue passage through the epithelial barrier induced by BSC damage. Since the IP concentration range selected for *in vitro* experiments was not based on the final concentration present in the esophagi, future efforts are required to validate these findings in animal model studies.

Moreover, we investigated about the ability of the IP to sustain the physiological repairing activity of human esophageal cells by improving and promoting the regenerative process of damaged esophageal mucosa. The results obtained highlighted the ability of the IP to induce a strong increase of wound healing and to reduce apoptosis induced by BSC. In addition, our results showed that the IP restored the physiological proliferation activity of CP-A cells previously stimulated with BSC.

Damaged mucosa is often associated with irritation and inflammation. Cytokines, in particular IL-6 and IL-8, are highly expressed in GERD patients [39]. In our model, CP-A and COLO-680 N cells responded to irritant stimulation (BSC), producing IL-6 and IL-8 cytokines. The pre-treatment of CP-A and COLO-680 N cells with the IP strongly reduced the production of these cytokines induced by BSC stimulation, confirming that the IP was able to create an effective barrier, preventing epithelial cell activation. In addition to this, an interesting characteristic of the IP was that it showed anti-inflammatory/soothing activities. Treatment with the IP of BSC-activated cells was able to reduce, in both cell types, IL-8 expression. This is an important property of the IP, since the suppression of IL-8, a chemoattractant of neutrophils to the site of inflammation, has been considered a target for the treatment of GERD patients [40]. The soothing and anti-inflammatory properties were attributable to the natural extract of germinated brown rice (Oryza sativa) present in the formulation of the IP.

5. Conclusions

Our data provide evidence that a new patented medical device, an oral formulation containing hyaluronic acid, rice extract, and amino acids dispersed in a bioadhesive polymer matrix, is able to strongly bind to human esophagus cells, improving the integrity of the mucosal barrier, and thus offering protection against the damaging effects of bile salts and pepsin on the esophageal mucosa. Thanks to its anti-irritative, soothing, and reparative properties observed during the study, the medical device may be used in combination with current medications for the management of gastroesophageal reflux that work through a different mechanism of action.

Funding

This research was supported by grants from the Institute for Maternal and Child Health, IRCCS "Burlo Garofolo", Trieste, Italy (RC 20/16, RC 23/18 to G.R. and 5MILLE15D to C.A.).

Declaration of Competing Interest

The authors report no declarations of interest.

Acknowledgments

We thank Dr. Cristina Bellarosa (Liver Research Center, Liver Foundation, Trieste, Italy) and Dr. Paolo Durigutto for providing the esophagi.

Appendix A. Supplementary data

Supplementary material related to this article can be found, in the online version, at doi:https://doi.org/10.1016/j.biopha.2020.110752.

References

[1] M.A. Menezes, F.A.M. Herbella, Pathophysiology of gastroesophageal reflux disease, World J. Surg. 41 (7) (2017) 1666–1671.
[2] J. Akiyama, S. Kuribayashi, M.K. Baeg, N. de Bortoli, E. Valitova, E.V. Savarino, M. Kusano, G. Triadafilopoulos, Current and future perspectives in the management of gastroesophageal reflux disease, Ann. N. Y. Acad. Sci. 1434 (1) (2018) 70–83.
[3] L.H. Eusebi, R. Ratnakumaran, Y. Yuan, M. Solaymani-Dodaran, F. Bazzoli, A. C. Ford, Global prevalence of, and risk factors for, gastro-oesophageal reflux symptoms: a meta-analysis, Gut 67 (3) (2018) 430–440.
[4] C. Body, J.A. Christie, Gastrointestinal diseases in pregnancy: nausea, vomiting, hyperemesis gravidarum, gastroesophageal reflux disease, constipation, and diarrhea, Gastroenterol. Clin. North Am. 45 (2) (2016) 267–283.
[5] R. Zielinski, K. Searing, M. Deibel, Gastrointestinal distress in pregnancy: prevalence, assessment, and treatment of 5 common minor discomforts, J. Perinat. Neonatal Nurs. 29 (1) (2015) 23–31.
[6] P. Usai Satta, F. Oppia, F. Cabras, Overview of pathophysiological features of GERD, Minerva Gastroenterol. Dietol. 63 (3) (2017) 184–197.
[7] J. Tack, J.E. Pandolfino, Pathophysiology of gastroesophageal reflux disease, Gastroenterology 154 (2) (2018) 277–288.
[8] R.C. Orlando, The integrity of the esophageal mucosa. Balance between offensive and defensive mechanisms, Best Pract. Res. Clin. Gastroenterol. 24 (6) (2010) 873–882.
[9] F.B. van Hoeij, P.W. Weijenborg, M.A. van den Bergh Weerman, R.M. van den Wijngaard, J. Verheij, A.J. Smout, A.J. Bredenoord, Mucosal integrity and sensitivity to acid in the proximal esophagus in patients with gastroesophageal reflux disease, Am. J. Physiol. Gastrointest. Liver Physiol. 311 (1) (2016) G117–22.
[10] R.F. Souza, The role of acid and bile reflux in oesophagitis and Barrett's metaplasia, Biochem. Soc. Trans. 38 (2) (2010) 348–352.
[11] D.O. Prichard, A.M. Byrne, J.O. Murphy, J.V. Reynolds, J. O'Sullivan, R. Feighery, B. Doyle, O.S. Eldin, S.P. Finn, A. Maguire, D. Duff, D.P. Kelleher, A. Long, Deoxycholic acid promotes development of gastroesophageal reflux disease and Barrett's oesophagus by modulating integrin-alphav trafficking, J. Cell. Mol. Med. 21 (12) (2017) 3612–3625.
[12] A. Zhao, S. Wang, W. Chen, X. Zheng, F. Huang, X. Han, K. Ge, C. Rajani, Y. Huang, H. Yu, J. Zhu, W. Jia, Increased levels of conjugated bile acids are associated with human bile reflux gastritis, Sci. Rep. 10 (1) (2020) 11601.
[13] D.S. Sandhu, R. Fass, Current trends in the management of gastroesophageal reflux disease, Gut Liver 12 (1) (2018) 7–16.
[14] M. Casale, A. Moffa, P. Vella, V. Rinaldi, M.A. Lopez, V. Grimaldi, F. Salvinelli, Systematic review: the efficacy of topical hyaluronic acid on oral ulcers, J. Biol. Regul. Homeost. Agents 31 (4 Suppl. 2) (2017) 63–69.
[15] Y. Liu, X. Wang, C.A. Hu, Therapeutic potential of amino acids in inflammatory bowel disease, Nutrients 9 (9) (2017).
[16] E. Kurtys, U.L.M. Eisel, R.J.J. Hageman, J.M. Verkuyl, L.M. Broersen, R. Dierckx, E. F.J. de Vries, Anti-inflammatory effects of rice bran components, Nutr. Rev. 76 (5) (2018) 372–379.
[17] N. Fedchenko, J. Reifenrath, Different approaches for interpretation and reporting of immunohistochemistry analysis results in the bone tissue - a review, Diagn. Pathol. 9 (2014) 221.
[18] C.T. Rueden, J. Schindelin, M.C. Hiner, B.E. DeZonia, A.E. Walter, E.T. Arena, K. W. Eliceiri, ImageJ2: ImageJ for the next generation of scientific image data, BMC Bioinf. 18 (1) (2017) 529.
[19] L. Cheng, W. Cao, C. Fiocchi, J. Behar, P. Biancani, K.M. Harnett, In vitro model of acute esophagitis in the cat, Am. J. Physiol. Gastrointest. Liver Physiol. 289 (5) (2005) G860–9.
[20] K. Kc, M.E. Rothenberg, J.D. Sherrill, In vitro model for studying esophageal epithelial differentiation and allergic inflammatory responses identifies keratin involvement in eosinophilic esophagitis, PLoS One 10 (6) (2015), e0127755.
[21] M.P. Di Simone, F. Baldi, V. Vasina, F. Scorrano, M.L. Bacci, A. Ferrieri, G. Poggioli, Barrier effect of Esoxx((R)) on esophageal mucosal damage: experimental study on ex-vivo swine model, Clin. Exp. Gastroenterol. 5 (2012) 103–107.
[22] A. Lanas, Y. Royo, J. Ortego, M. Molina, R. Sainz, Experimental esophagitis induced by acid and pepsin in rabbits mimicking human reflux esophagitis, Gastroenterology 116 (1) (1999) 97–107.
[23] K.G. Pursnani, M.A. Mohiuddin, K.R. Geisinger, G. Weinbaum, D.A. Katzka, D. O. Castell, Experimental study of acid burden and acute oesophagitis, Br. J. Surg. 85 (5) (1998) 677–680.
[24] O.J. Kwon, M.Y. Kim, S.H. Shin, A.R. Lee, J.Y. Lee, B.I. Seo, M.R. Shin, H.G. Choi, J. A. Kim, B.S. Min, G.N. Kim, J.S. Noh, M.H. Rhee, S.S. Roh, Antioxidant and anti-inflammatory effects of Rhei Rhizoma and Coptidis Rhizoma mixture on reflux esophagitis in rats, Evid. Complement. Alternat. Med. 2016 (2016), 2052180.
[25] D.C. Gotley, A.P. Morgan, D. Ball, R.W. Owen, M.J. Cooper, Composition of gastro-oesophageal refluxate, Gut 32 (10) (1991) 1093–1099.
[26] K. Blondeau, A. Pauwels, L. Dupont, V. Mertens, M. Proesmans, R. Orel, J. Brecelj, M. Lopez-Alonso, M. Moya, A. Malfroot, E. De Wachter, Y. Vandenplas, B. Hauser, D. Sifrim, Characteristics of gastroesophageal reflux and potential risk of gastric content aspiration in children with cystic fibrosis, J. Pediatr. Gastroenterol. Nutr. 50 (2) (2010) 161–166.
[27] H.J. Sung, Y.K. Cho, S.J. Moon, J.S. Kim, C.H. Lim, J.M. Park, I.S. Lee, S.W. Kim, M. G. Choi, Role of Acid and weakly acidic reflux in gastroesophageal reflux disease off proton pump inhibitor therapy, J. Neurogastroenterol. Motil. 18 (3) (2012) 291–297.
[28] S. Emerenziani, M. Ribolsi, M.P. Guarino, P. Balestrieri, A. Altomare, M.P. Rescio, M. Cicala, Acid reflux episodes sensitize the esophagus to perception of weakly acidic and mixed reflux in non-erosive reflux disease patients, Neurogastroenterol. Motil. 26 (1) (2014) 108–114.
[29] N. de Bortoli, A. Ottonello, F. Zerbib, D. Sifrim, C.P. Gyawali, E. Savarino, Between GERD and NERD: the relevance of weakly acidic reflux, Ann. N. Y. Acad. Sci. 1380 (1) (2016) 218–229.
[30] A.F. Hofmann, L.R. Hagey, Key discoveries in bile acid chemistry and biology and their clinical applications: history of the last eight decades, J. Lipid Res. 55 (8) (2014) 1553–1595.
[31] A.F. Hofmann, K.J. Mysels, Bile acid solubility and precipitation in vitro and in vivo: the role of conjugation, pH, and Ca2+ ions, J. Lipid Res. 33 (5) (1992) 617–626.
[32] D. Nehra, P. Howell, C.P. Williams, J.K. Pye, J. Beynon, Toxic bile acids in gastro-oesophageal reflux disease: influence of gastric acidity, Gut 44 (5) (1999) 598–602.
[33] R. Farre, H. van Malenstein, R. De Vos, K. Geboes, I. Depoortere, P. Vanden Berghe, F. Fornari, K. Blondeau, V. Mertens, J. Tack, D. Sifrim, Short exposure of oesophageal mucosa to bile acids, both in acidic and weakly acidic conditions, can impair mucosal integrity and provoke dilated intercellular spaces, Gut 57 (10) (2008) 1366–1374.
[34] R.C. Orlando, D.W. Powell, C.N. Carney, Pathophysiology of acute acid injury in rabbit esophageal epithelium, J. Clin. Invest. 68 (1) (1981) 286–293.
[35] S. Bor, D. Capanoglu, The additive effect of ethanol and extract of cigarette smoke on rabbit esophagus epithelium, J. Gastroenterol. Hepatol. 24 (2) (2009) 316–321.
[36] L.A. Blackshaw, D.S. Bordin, C. Brock, A. Brokjaer, A.M. Drewes, A.D. Farmer, A. L. Krarup, C. Lottrup, A.A. Masharova, F.J. Moawad, A.E. Olesen, Pharmacologic treatments for esophageal disorders, Ann. N. Y. Acad. Sci. 1325 (2014) 23–39.
[37] M. Tang, P. Dettmar, H. Batchelor, Bioadhesive oesophageal bandages: protection against acid and pepsin injury, Int. J. Pharm. 292 (1–2) (2005) 169–177.
[38] H.K. Batchelor, M. Tang, P.W. Dettmar, F.C. Hampson, I.G. Jolliffe, D.Q. Craig, Feasibility of a bioadhesive drug delivery system targeted to oesophageal tissue, Eur. J. Pharm. Biopharm. 57 (2) (2004) 295–298.
[39] H. Isomoto, K. Inoue, S. Kohno, Interleukin-8 levels in esophageal mucosa and long-term clinical outcome of patients with reflux esophagitis, Scand. J. Gastroenterol. 42 (3) (2007) 410–411.
[40] N. Yoshida, Inflammation and oxidative stress in gastroesophageal reflux disease, J. Clin. Biochem. Nutr. 40 (1) (2007) 13–23.